

June 16, 2010

To:

Prof. Dr. Dennis Baldocchi
University of California, Berkeley
Dept of Environmental Science, Policy and Management
345 Hilgard Hall
Berkeley, CA 94720

From:

Dr. Andres Schmidt
Department of Forest Ecosystems and Society
AmeriFlux QA/QC Lab
Oregon State University
Corvallis, OR 97331

Dear Prof. Dr. Baldocchi,

Thank you for your cooperation and support during the comparison between your eddy covariance system at the AmeriFlux Tonzi Ranch site, California (hereafter referred to as US-Ton) and the AmeriFlux Portable eddy covariance system (hereafter referred to as AmeriFlux PS) from May 13 through May 22, 2010. During the measurements used for the comparison the AmeriFlux PS sensors were setup at a reasonable distance to foster comparability of the results while also minimizing flow distortions or shadowing effects caused by the additional sensors. Radiation sensors were attached alongside the US-Ton radiation sensors, both orientated to the south at the same height with a horizontal distance of 60 cm. The AmeriFlux PS EC system was orientated to the West at a height of 21.7 m (a.g.l.). The vertical distance between the two anemometers was 90 cm. The horizontal distance of the AmeriFlux sonic anemometer to the US-Ton sonic anemometer was 70 cm. The aspirated AmeriFlux PS temperature sensor was installed at the top of the tower next to the US-Ton temperature sensor in a horizontal distance of 1.2 m.

To assure a reliable data quality for the reference dataset, the AmeriFlux PS flux estimates are automatically flagged depending on stationarity and developed turbulent conditions for the complete comparison period. Furthermore, plausibility limits for all sensor readings were applied. As a result of the objective QA/QC routines, you may see some data gaps occurring in our time series as low-quality data were automatically excluded from the comparison. Furthermore, outliers and readings with errors were also excluded from both data sets to remove major spikes in order to get meaningful results for the final linear regression analyses. In general, the comparisons yielded a good agreement between the two. Please see the part of the report related to the meteorological variables for details. The regression analyses and the time series comparison of the measured variables have been included in this report. Below you will find the figures and details of the comparison and the suggested interpretation.

Summary of recommendations

- A check of the temperature sensor is recommended. If the calibration and performance of the HMP sensor turn out to be correct we recommend that you mount the sensor at a position which is less exposed to the south to avoid radiation disturbances on the temperature measurements as far as possible.
- The sonic temperature was off by 18% on average from the AmeriFlux CSAT3 sensor (calibrated December 02 2009). Please check the calibration of the WindMaster Pro. Also problems with the firmware of the WindmasterPro have been reported (see PDF attached to the email). There is a new version available which fixes the known problems of the WindMaster pro with the speed of sound and the sonic temperature, respectively.

- Conduct routine maintenance and periodic *in-situ* field calibrations to assure the IRGA's good performance.

Please feel free to provide a response to this report with a description of how the recommendations will be incorporated. Thanks again for your help and collaboration.

Best regards,

Andres Schmidt

Observations

Meteorological Data (Fig. 1 – 10)

On average the mean horizontal wind speed measured with the WindMaster Pro of the *US-Ton* system is slightly higher than the resulting wind velocity measured with the CSAT3 of the AmeriFlux PS ($y=1.03x+0.05$, $R^2=0.99$, Fig.1). Derived wind directions generally compared well ($y=1.00x+0.94$, $R^2=1.00$, Fig. 2). All wind direction data were adjusted for geomagnetic declination which was $14^{\circ}12'$ E during the comparison period at the US-Ton site. No significant flow disturbance effects caused by the instrumentation could be determined. Also the variances of the rotated vertical wind vector component w used for the flux calculations match well with $R^2=1.00$ and no offset (Fig. 3).

The regression line of the derived friction velocity values shows a slope of 0.97 but no intercept. The sonic temperature measured by the US-Ton Gill WindMaster Pro shows significant differences to the sonic temperature values of the AmeriFlux PS CSAT3 ($y=0.82X+4.02$, $R^2=0.99$, Fig. 5). However, the variances of the sonic temperatures, that can be used to calculate buoyancy fluxes, match very well with no slope and no intercept for the linear regression (Fig. 6). Air temperature measured with the US-Ton HMP sensor tracks the temperature values of the aspirated AmeriFlux PS PT100 sensor. Nevertheless, the regression function exhibits a slope of 1.06. Figure 7 shows that the air temperature differences occur during noontime with the highest incoming radiation. Thus, it can be stated that the differences are caused by the heating of the HMP sensor. During noontime the radiation shield is not sufficient to prevent radiation effects on the measured temperature completely whereas the aspirated PT 100 sensor is not affected by these overheating effects. On May 17 with clouds and lower incoming radiation these effects do not occur (Fig. 7) which supports the assumption that the temperature differences are attributed to radiation effects on the US-Ton HMP sensor.

The atmospheric pressure values correlate well with $R^2=0.99$ with an intercept of only 0.21 kPa for the linear regression. Also the relative humidity measurements match the estimates from the AmeriFlux portable system. Observed offset and scatters are both small (Fig. 8). Derived VPD values determined by the *US-Ton* system were on average 2% higher in comparison to the respective values of the AmeriFlux PS (Fig. 10).

Gas concentrations (Fig. 11 – 14)

In order to yield reliable and accurate results for the water vapor and CO₂ volume concentrations the *AmeriFlux* PS IRGA LI-COR 7500 and LI-COR 7200 (backup system) were both calibrated at the beginning of the comparison period on 5/14/2010. Since the *US-Ton* system was equipped with an open-path sensor, the comparisons are based on the LI7500 values.

The mean CO₂ concentrations of the *US-Ton* LI7500 are on average 2% lower than the respective AmeriFlux PS LI7500 data causing a slope of 0.98 and an offset of 0.3 $\mu\text{mol m}^{-3}$ (Fig. 11). The variances of the CO₂ concentrations of the two open-path IRGAs are also in good agreement, the regression function shows no significant offset ($y=0.98X+0$, $R^2=0.99$, Fig. 12). The comparison of the water vapor concentration samples with those of the *AmeriFlux* open-path IRGA is satisfying ($y=0.99x+0.06$, $R^2=0.99$, Fig. 13) as well as the variances of the H₂O_g concentrations (Fig. 14). The good agreements of the variances of the CO₂ and water vapor concentrations (Fig. 12, Fig. 14) indicate that the *US-Ton* LI7500 was capable to catch the fluctuation of the scalars for reliable flux estimates during the analyzed comparison period.

Flux variables (Fig. 15 - 18)

The uncorrected covariance of the rotated vertical wind velocity and the carbon dioxide concentrations from the *US-Ton* system showed differences of 1% in comparison to the *AmeriFlux PS* data (Fig.15). So do the WPL corrected final fluxes of CO₂ ($y=0.99x-0.09$, $R^2=0.97$, Fig. 16).

The sensible heat fluxes H differ by 3%. The corresponding correlation between the values measured with the *US-Ton* system and those measured with the *Ameriflux PS* is very high ($R^2=1.0$). In comparison to the *AmeriFlux PS* values the sensible heat flux is slightly overestimated by 3.08 Wm⁻² on average as shown by the regression equation given in Figure 17. The comparison of the latent heat fluxes show a slope of 0.97 and an offset of 2.49 Wm⁻² and a regression coefficient of $R^2=0.99$ (Fig. 18).

Radiation (Fig. 19 – 21)

In general all observed radiation values measured with the *US-Ton* system from May 13 through May 22 agree very well with the corresponding values measured with the *AmeriFlux PS*. The total net radiation derived from the incoming and outgoing longwave radiation values and shortwave radiation values compared very well within 1% between your CNR1 sensor and our CNR1 sensor (Fig. 19). This also accounts for the averaged global radiation measurements ($y=0.99x-1.26$, $R^2=1.00$, Fig. 20). The regression function of the incoming photosynthetic active radiation (PAR) exhibits a slope of 1 and a negligible offset of 3.65 μmol m⁻² s⁻¹ (Fig. 21).

Figures of the AmeriFlux site intercomparison at Tonzi Ranch, 2010:

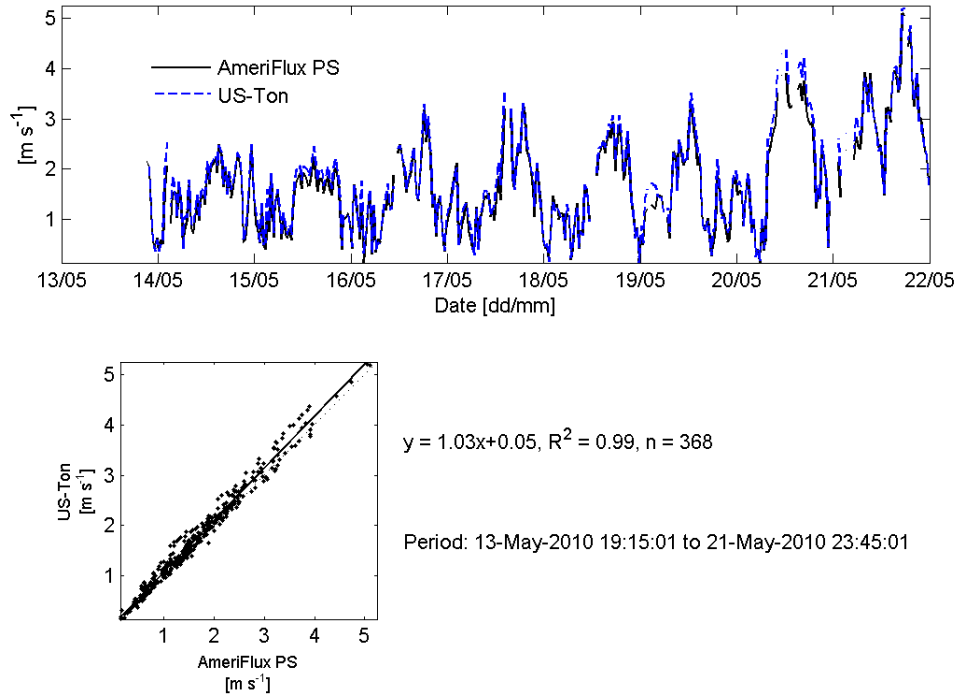


Figure 1: Resulting mean wind

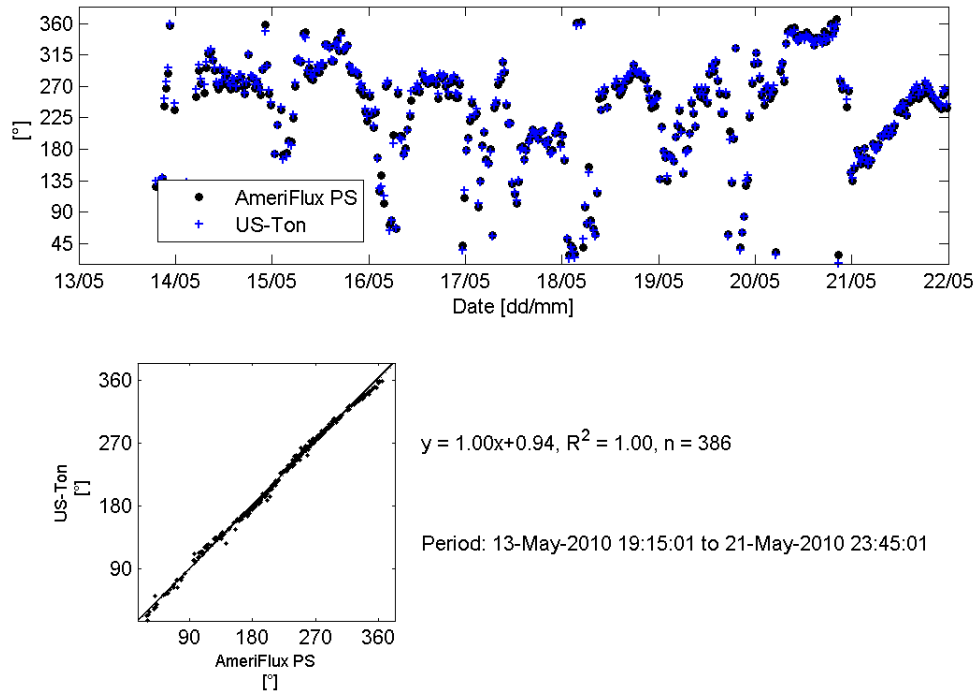


Figure 2: Mean wind direction

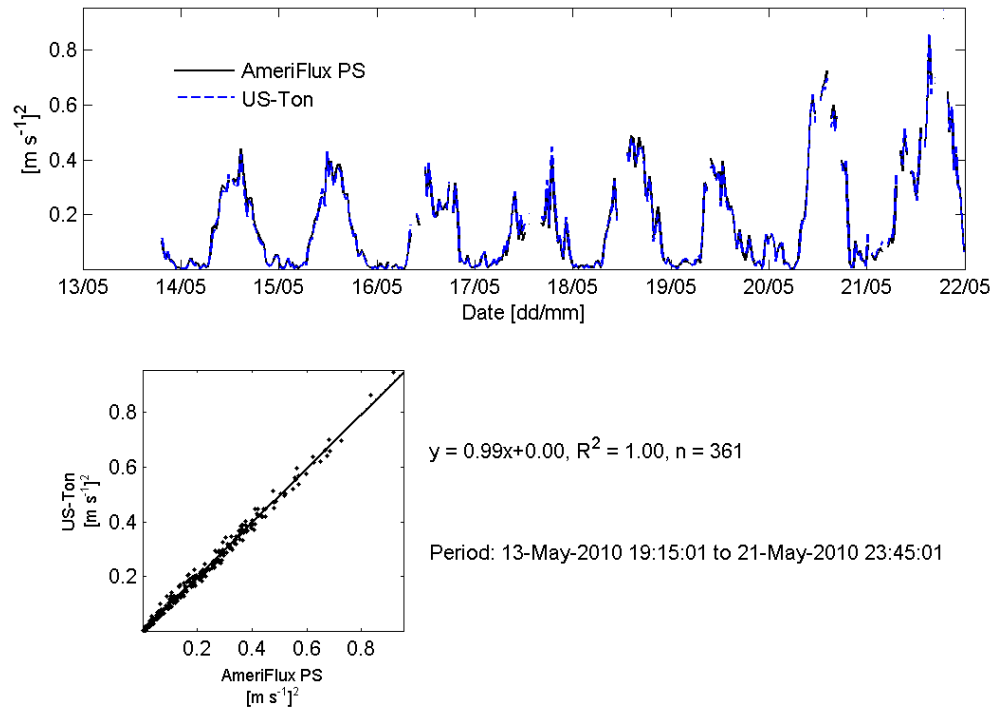


Figure 3: Variance of w

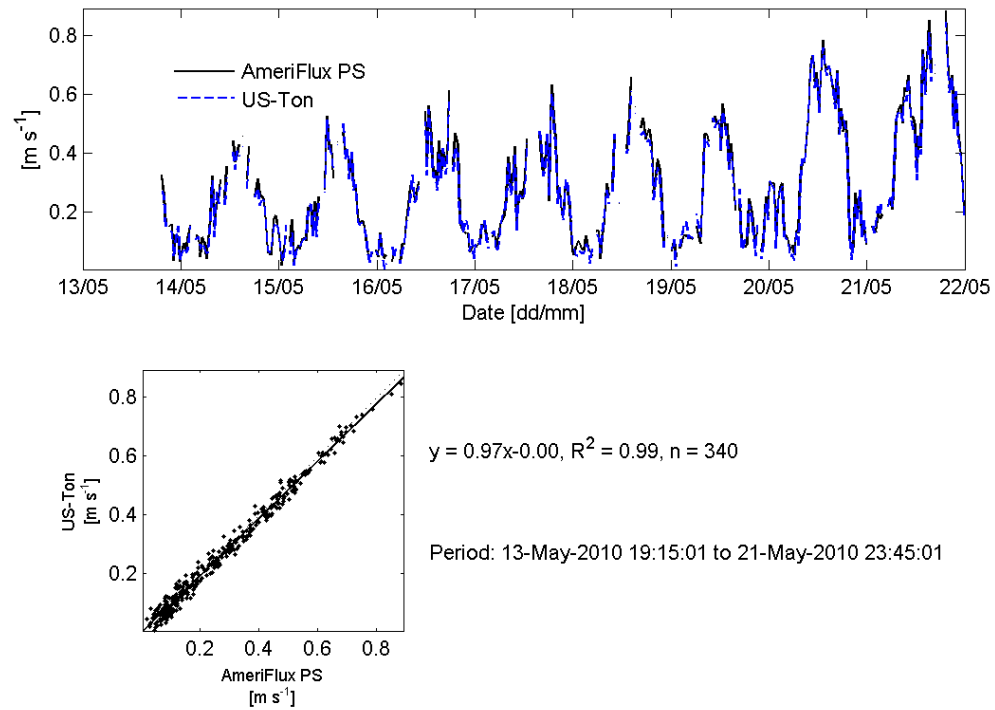
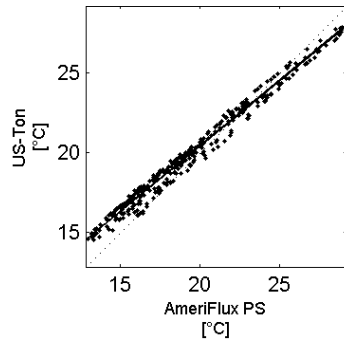
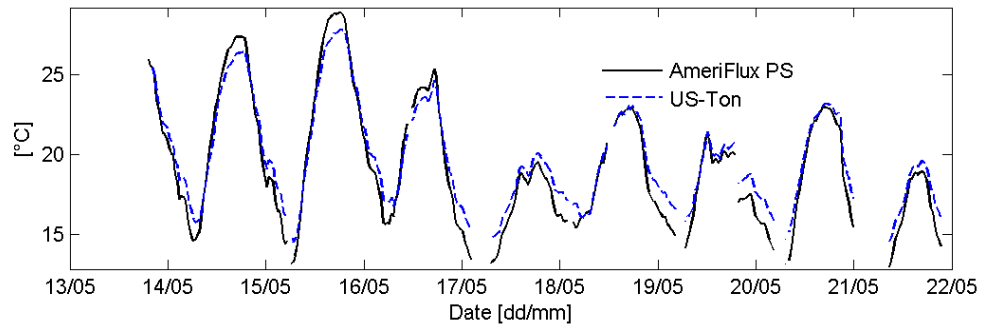


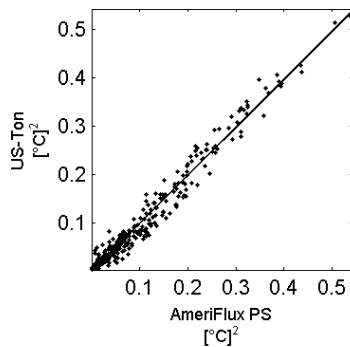
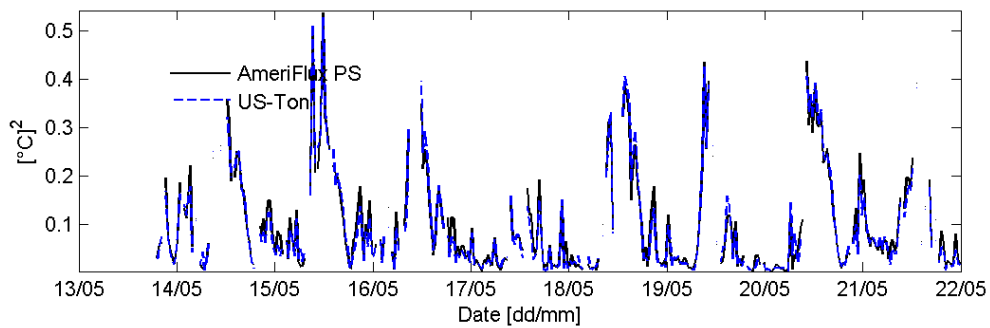
Figure 4: Friction velocity



$$y = 0.82x + 4.02, R^2 = 0.99, n = 346$$

Period: 13-May-2010 19:15:01 to 21-May-2010 23:45:01

Figure 5: Mean sonic temperature



$$y = 1.00x - 0.00, R^2 = 0.99, n = 341$$

Period: 13-May-2010 19:15:01 to 21-May-2010 23:45:01

Figure 6: Variance of sonic temperature

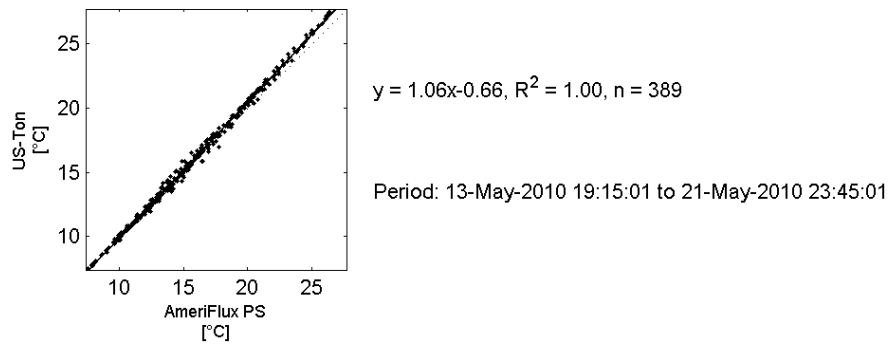
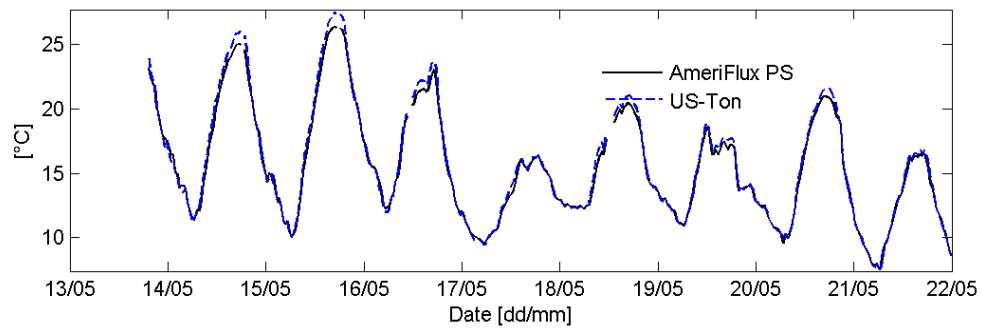


Figure 7: Air temperature

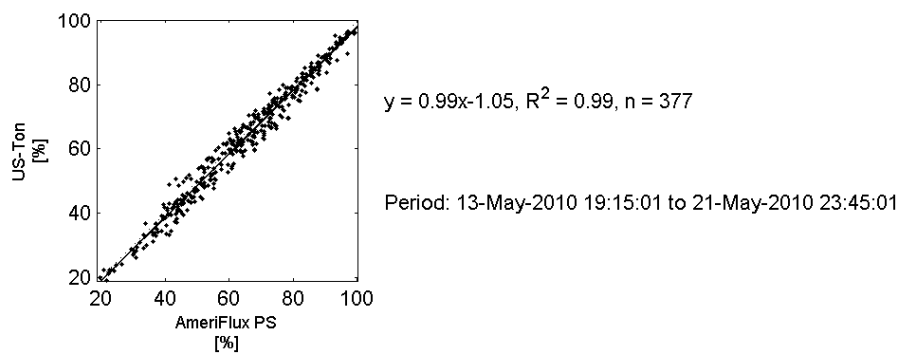
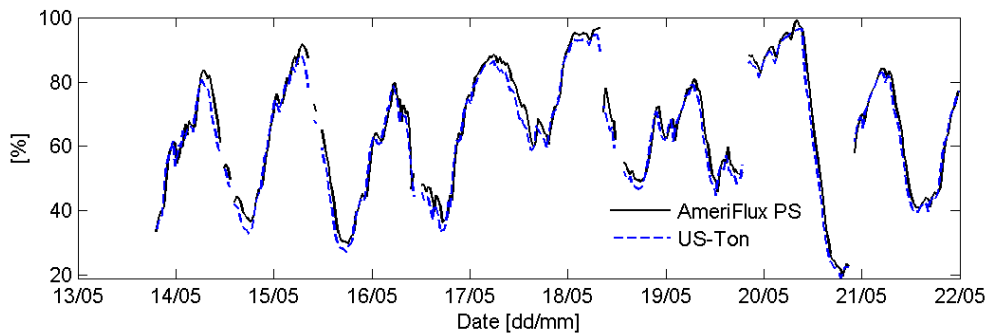


Figure 8: Relative humidity

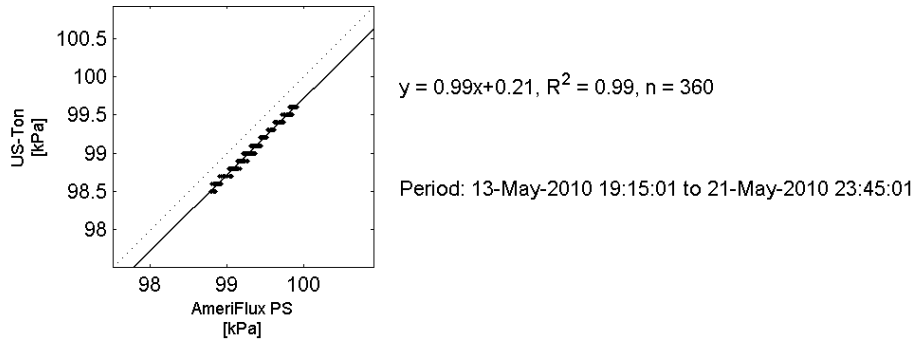
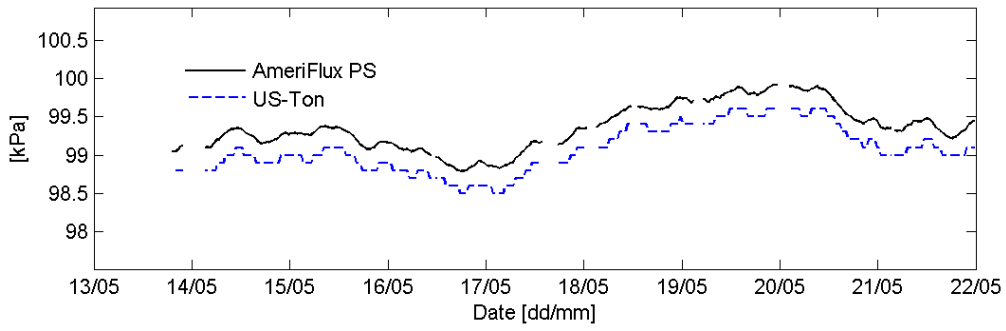


Figure 9: Atmospheric pressure

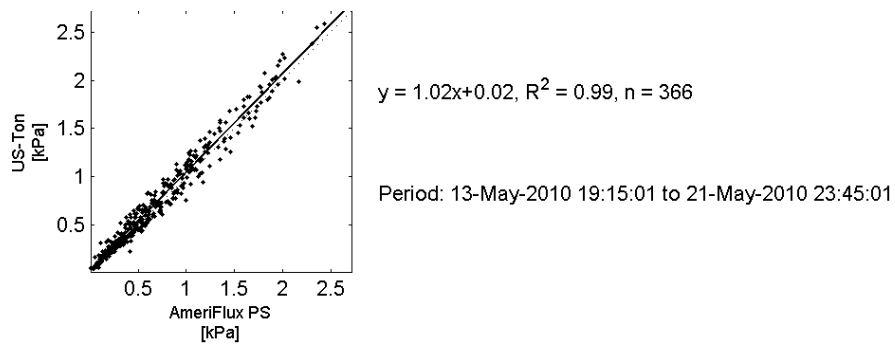
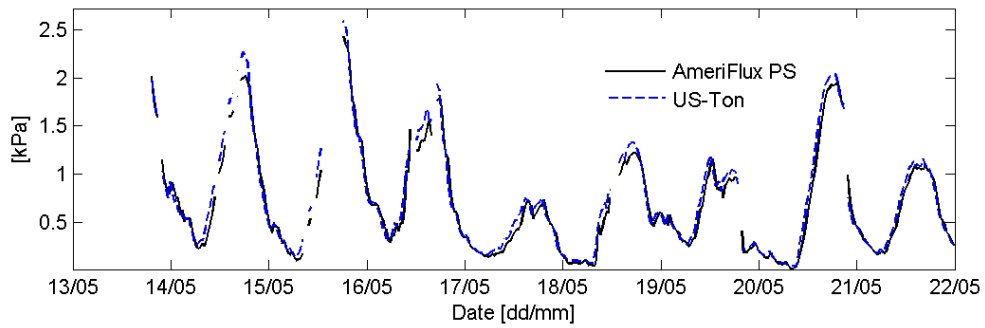


Figure 10: Vapor pressure deficit

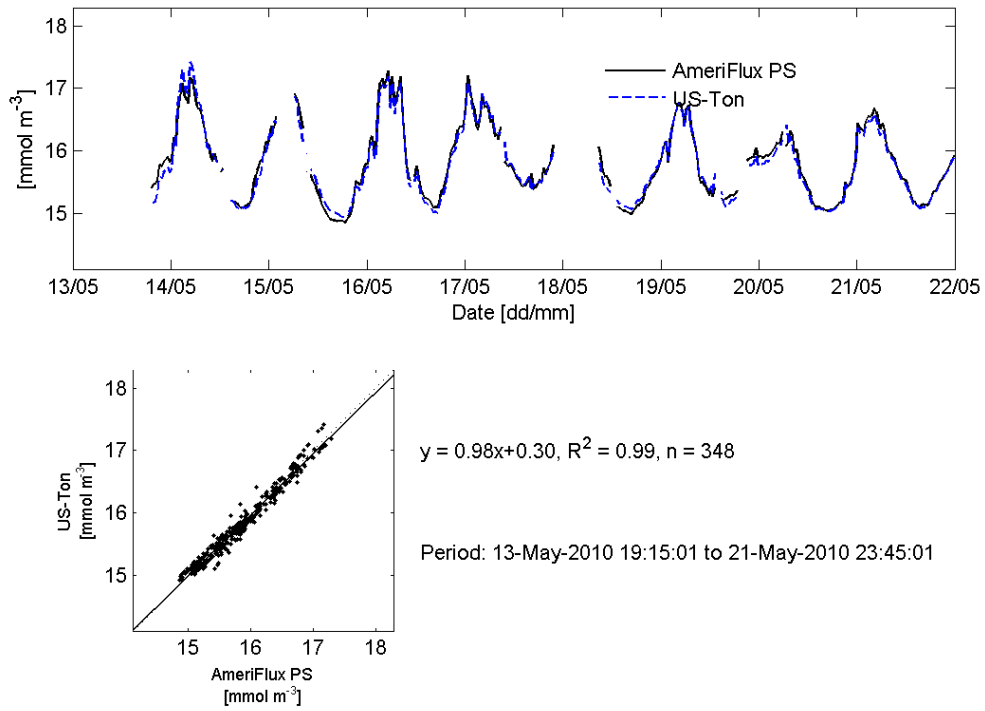


Figure 11: Mean carbon dioxide concentration

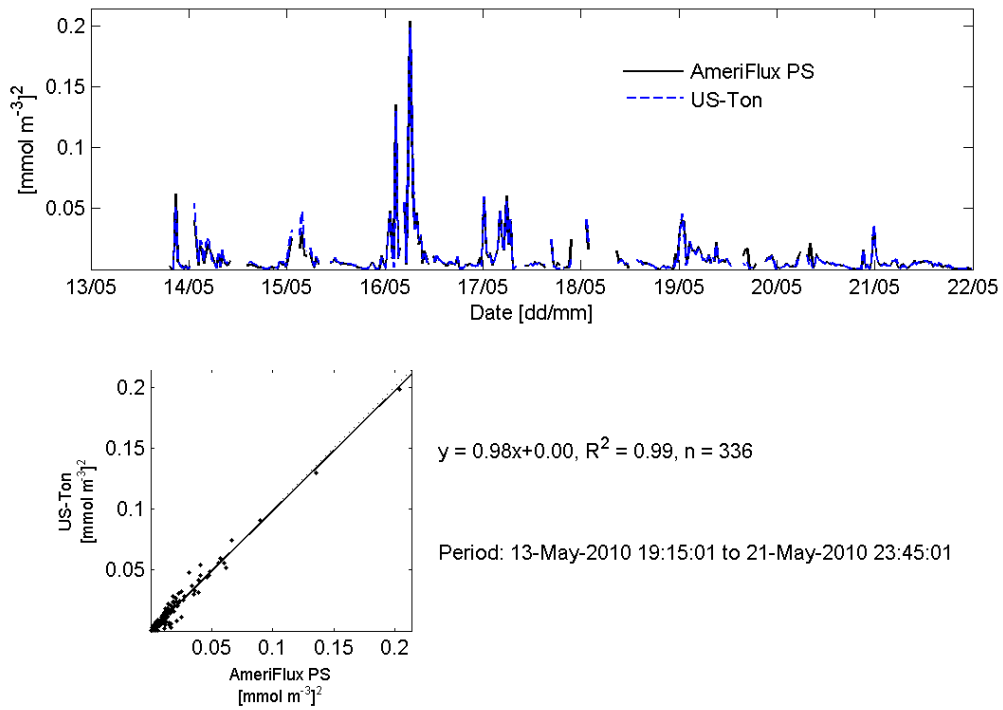


Figure 12: Variance of carbon dioxide concentration

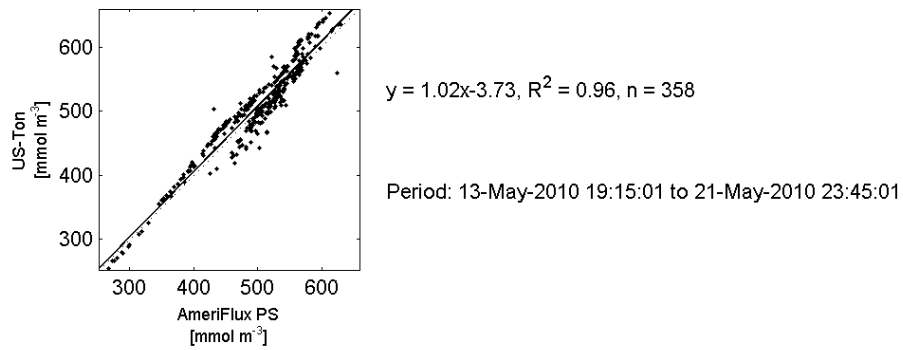
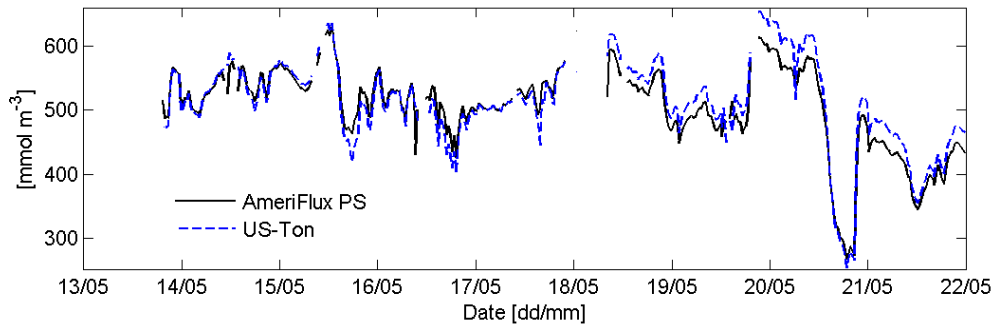


Figure 13: Mean water vapor concentration

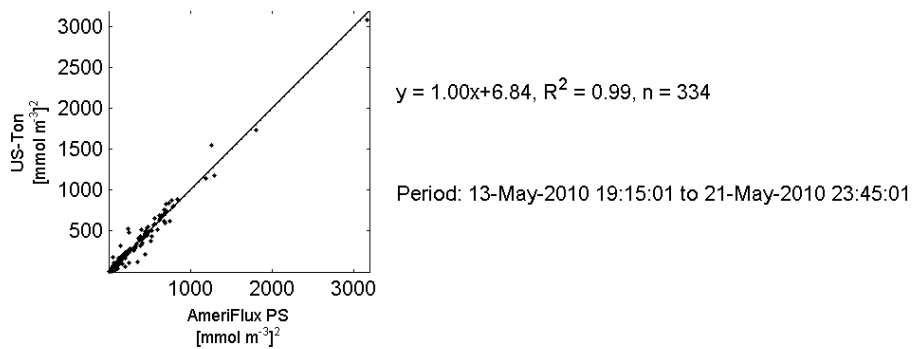
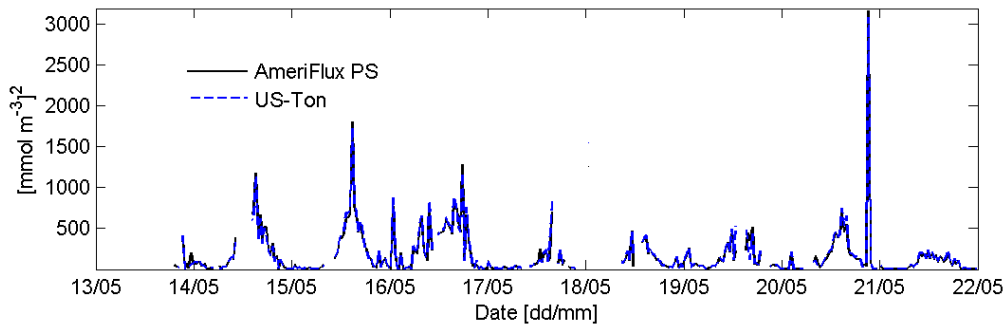


Figure 14: Variance of water vapor concentration

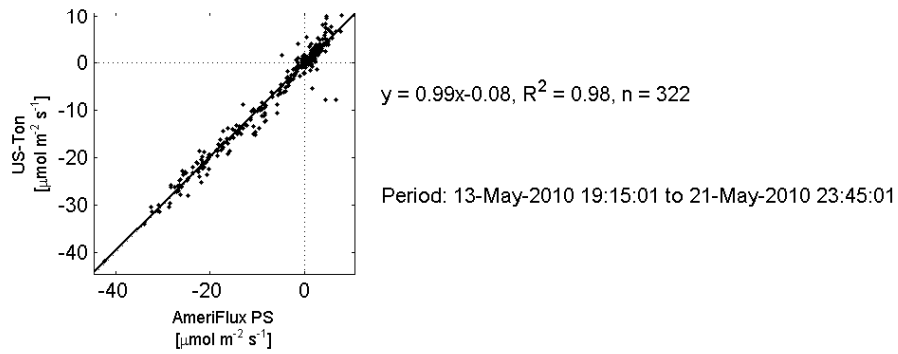
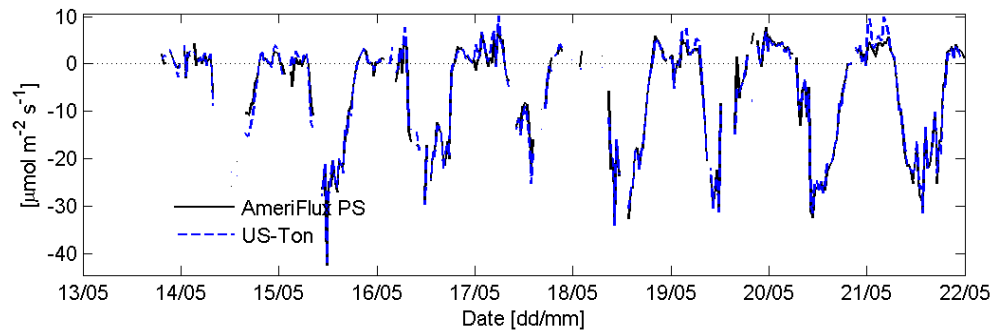


Figure 15: Raw covariance wCO_2

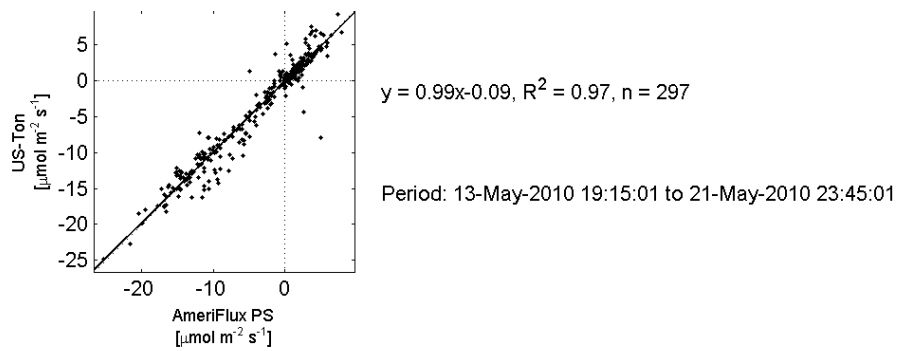
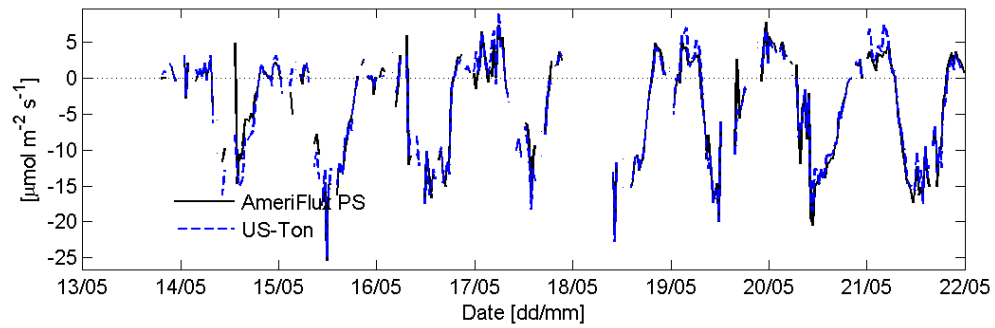


Figure 16: Carbon dioxide flux

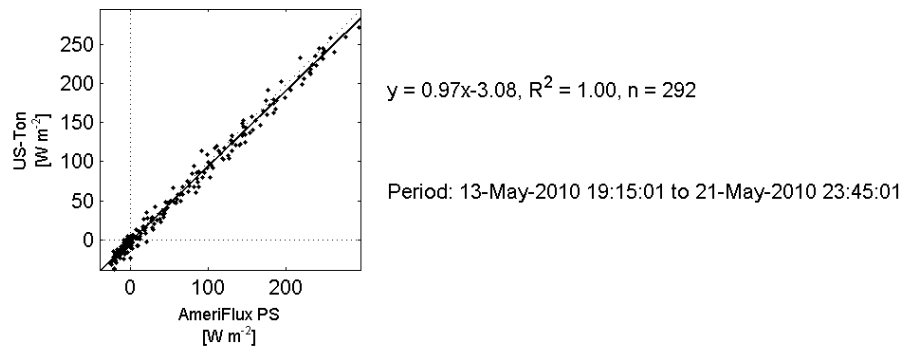
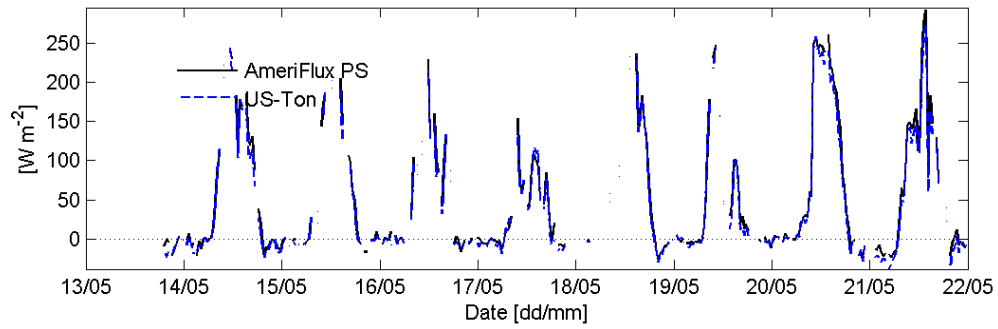


Figure 17: Sensible heat flux

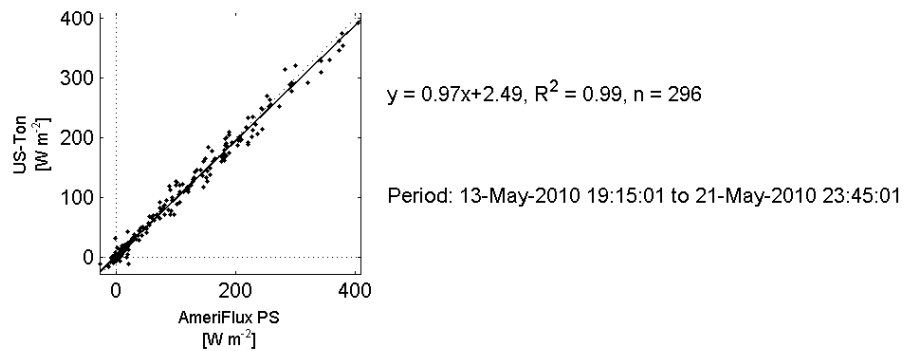
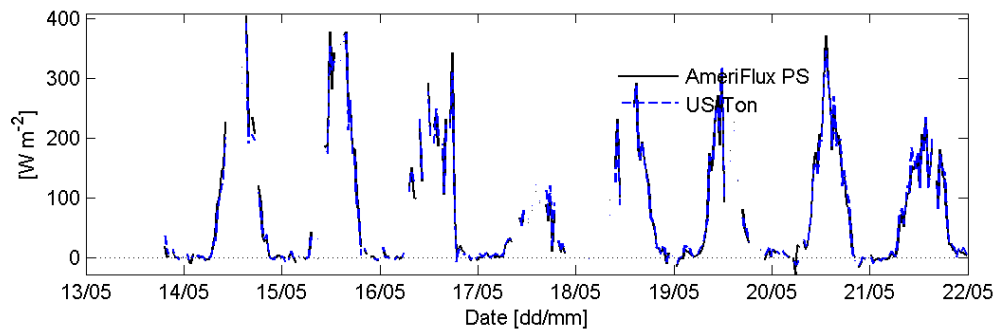


Figure 18: Latent heat flux

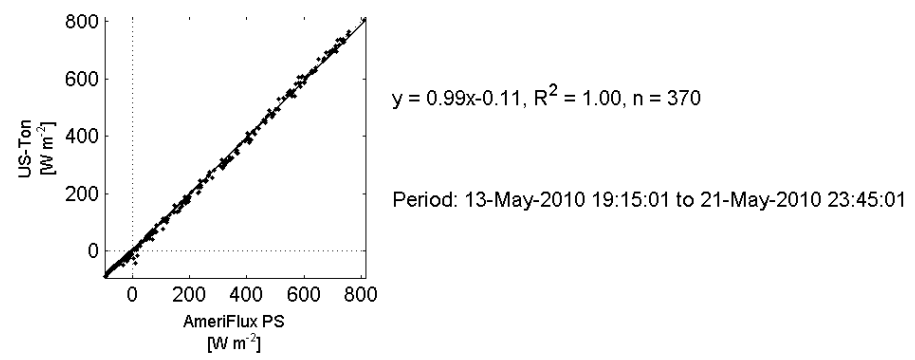
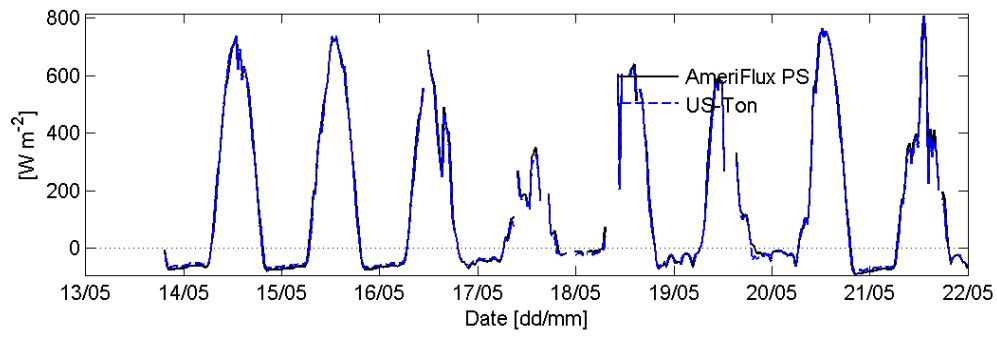


Figure 19: Net radiation

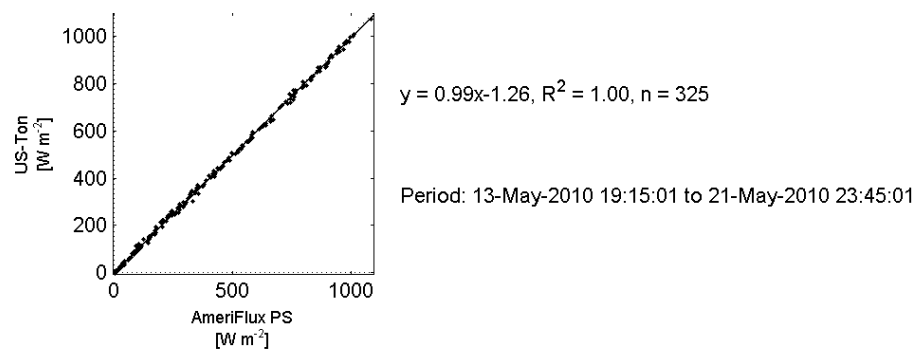
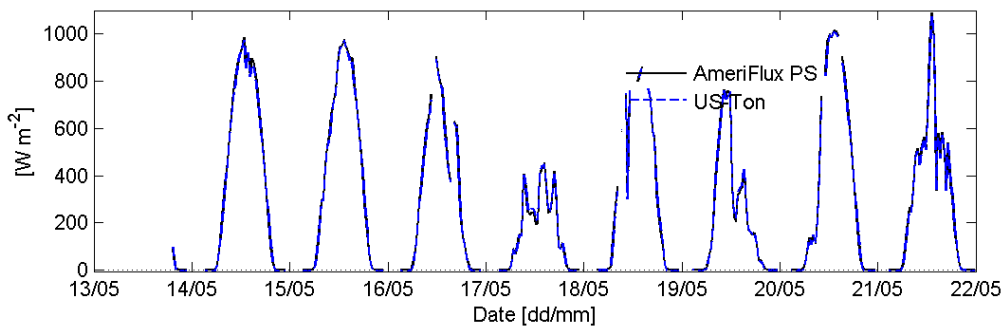
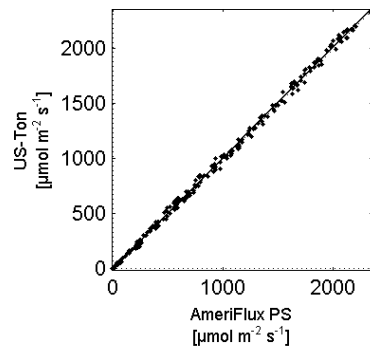
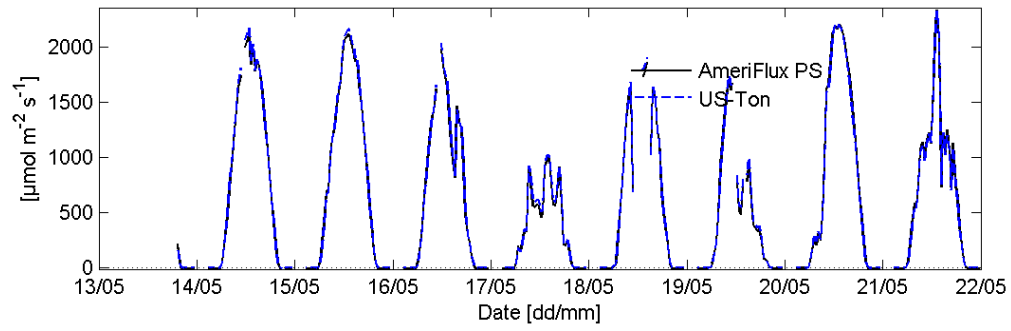


Figure 20: Global radiation



$$y = 1.00x + 3.65, R^2 = 1.00, n = 336$$

Period: 13-May-2010 19:15:01 to 21-May-2010 23:45:01

Figure 21: Incoming PAR